

Lattice QCD Overview

Attila Pásztor^{1,2,*}

¹Institute for Theoretical Physics, Eötvös Loránd University, Pázmány P. stny. 1/A, H-1117, Budapest

²HUN-REN-ELTE Theoretical Physics Research Group, Pázmány P. stny. 1/A, H-1117 Budapest

Abstract. I review recent progress in lattice QCD calculations of the QCD phase diagram and equation of state at non-zero temperature and baryochemical potential. I also discuss some connections with heavy ion collisions.

1 Introduction

The study of QCD under extreme conditions has been a very active field of research for decades. In particular, the study of the phase diagram in the temperature (T)-baryochemical potential (μ_B) plane has garnered lots of interest by both the experimental and theoretical communities. Lattice QCD calculations have been very important in this quest, as lattice can deliver fully non-perturbative results in full QCD. Indeed, lattice results on QCD matter have been influential. Lattice QCD has shown [1], that the deconfinement/chiral transition at $\mu_B = 0$ is not a true phase transition, but rather a smooth crossover. Furthermore, the equation of state at $\mu_B = 0$ is also well established [2–4]. At $\mu_B > 0$, model calculations predict a critical endpoint [5–9], where the crossover line becomes a line of first order transitions. Locating the position of this critical endpoint (CEP) is a main goal of heavy ion physics. First principle lattice QCD simulations at $\mu_B > 0$ are hampered by a sign problem. Thus, most results on physics at $\mu_B > 0$ come from extrapolations. Either from Taylor coefficients at $\mu_B = 0$, or from results at purely imaginary chemical potentiala, i.e., $\mu_B^2 \leq 0$. Here, I discuss results on the transition line and the width of the crossover at $\mu_B \geq 0$, baryon number fluctuations, as well as the equation of state, isentropes and critical lensing.

2 The transition temperature and width at small μ_B

The value of the crossover temperature at $\mu_B = 0$ is well established [10, 11]. A recent, precise calculation [12] gives $T_c(\mu_B = 0) = 158.0 \pm 0.6$ MeV. This value approximately agrees with (or is maybe slightly higher than) the chemical freeze-out temperature extracted from heavy ion collision data at higher collision energies [13–16], in accordance with expectations [17]. At $\mu_B > 0$, the crossover temperature is usually written as a Taylor expansion:

$$\frac{T_c(\mu_B)}{T_c(0)} = 1 - \kappa_2 \left(\frac{\mu_B}{T_c(\mu_B)} \right)^2 - \kappa_4 \left(\frac{\mu_B}{T_c(\mu_B)} \right)^4 + \dots \quad (1)$$

The expansion is written in terms of $\mu_B/T_c(\mu_B)$ and not μ_B due to technical convenience on the lattice, but the coefficients κ_2 and κ_4 can be easily converted to Taylor coefficients in

*e-mail: apasztor@bodri.elte.hu

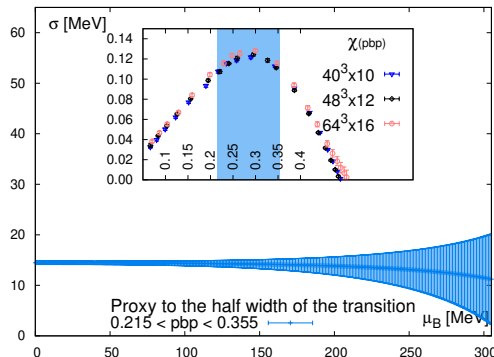


Figure 1. Extrapolation of the width of the crossover transition to real μ_B .

the chemical potential μ_B itself [18]. For the κ_2 coefficient, calculations by three different lattice groups, using both the imaginary chemical potential and Taylor methods are in good agreement [12, 19–22]. For the κ_4 coefficient, there are two calculations at the moment, one with the Taylor method [22], and the other with the imaginary chemical potential method [12]. The most precise determination of the κ_2 and κ_4 coefficients - based on the chiral condensate - is given in Ref. [12] as $\kappa_2 = 0.0153 \pm 0.0018$ and $\kappa_4 = 0.00032 \pm 0.00067$. Thus, the transition line on the phase diagram is - to a very good approximation - a parabola. A joint Bayesian analysis [18] of the Taylor coefficient data of Ref. [22] and the imaginary chemical potential data of Ref. [12] suggest that the transition line can be well approximated with a parabola in μ_B (but not in $\mu_B/T_c(\mu_B)$) up to chemical potentials as high as $\mu_B \approx 600$ MeV. At large μ_B the chemical freeze-out curve is expected to approach the nuclear-liquid gas critical point [23] and not the chiral CEP. Thus, the chiral transition curve and the freeze-out curve should deviate at some value of μ_B . Where and how this deviation happens is an important open question.

Knowing the $T_c(\mu_B)$ curve does not automatically lead to a determination of the position of the CEP. For that purpose, other observables have to be considered. One possibility is the width of the transition: Since the transition at $\mu_B = 0$ is a crossover, there is no non-analyticity in the free energy, and thus no sharp point of transition. Rather, there is an extended transition region in T , which can be characterized with a width parameter. One definition of a width parameter σ is given in Ref. [12], where this width parameter was extrapolated to real μ_B using the imaginary chemical potential method. The results are shown in Fig. 1. σ going to zero would indicate the presence of a CEP. The results show that for small μ_B the width σ is approximately constant: The transition does not get narrower below the value of $\mu_B \approx 300$ MeV. Another way to see the approximately constant width of the crossover is through the existence of an approximate scaling variable [24–26]. The existence of this approximate scaling variable is illustrated in Fig. 2, where the baryon-density-to-chemical potential ratio $\chi_1^B/(\mu_B/T)$ is plotted as a function of T (left panel) and as a function of $T \left(1 + \kappa_2 \left(\frac{\mu_B}{T}\right)^2\right)$ (right panel). The curvature of the transition line ¹. Thus, Figs. 1 and 2 tell the same story: the story of a crossover transition whose temperature depends on the chemical potential, but its width does not. What happens with the width of the transition at larger μ_B is an open question.

¹The numerical value of κ_2 in Section 2 and in Figure 2 is different, because in Section 2, the result is quoted for the phenomenologically most relevant case of strangeness neutrality $n_S = 0$, while Figure 2 is for illustration purposes only, and uses the simpler case of zero strangeness chemical potential $\mu_S = 0$.

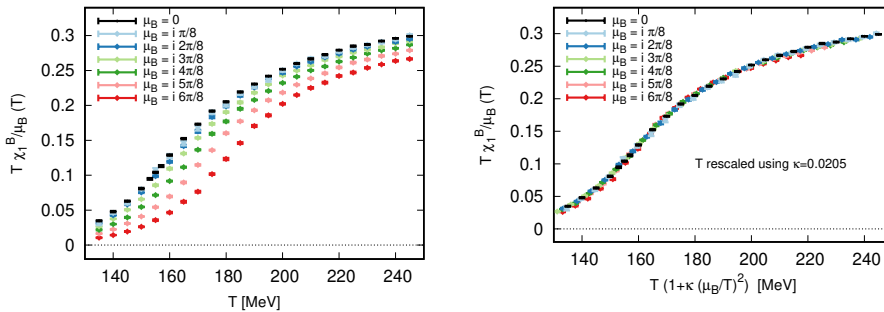


Figure 2. Collapse plot for the baryon density-to-chemical potential ratio.

3 Baryon number fluctuations

An important set of quantities are the generalized susceptibilities of the baryon number: derivatives of the pressure with respect to μ_B , written as $\chi_n^B(T, \mu_B) = \frac{\partial(p/T^4)}{\partial^n(\mu_B/T)^n}$. Evaluating these at $\mu_B = 0$ is possible, and allows for a Taylor expansion of the pressure:

$$\frac{p(T, \mu_B) - p(0, \mu_B)}{T^4} = \frac{1}{2!} \chi_2^B(T, 0) \left(\frac{\mu_B}{T} \right)^2 + \frac{1}{4!} \chi_4^B(T, 0) \left(\frac{\mu_B}{T} \right)^4 + \dots \quad (2)$$

Differentiation of the above formula allows for a Taylor expansion of the susceptibilities $\chi_n^B(T, \mu_B)$ also, with the coefficients also given by $\chi_n^B(T, 0)$. The coefficients $\chi_n^B(T, \mu_B = 0)$ are thus important for several applications, such as the extrapolation of the equation of state to $\mu_B > 0$, extrapolation of susceptibilities to search for signs of criticality, to probe the effective degrees of freedom of QCD matter [27–29] or to study chemical freeze-out in heavy ion collisions (for the difficulties in comparing with experiments, see, e.g., Refs. [30–32]).

The lattice QCD community has spent considerable effort in calculating these coefficients. The highest order coefficient available from the lattice is χ_8^B [33–37]. In Fig. 3 three different lattice QCD results are shown for the the coefficients χ_6^B and χ_8^B . The green bands are results of the HotQCD collaboration [36], using the Taylor method and a coarser lattice, with 8 timeslices. The black points are results from the Wuppertal-Budapest collaboration [34], using the imaginary chemical potential method, on a finer lattice, with 12 timeslices. Finally, the orange bands shows recent results from the Wuppertal-Budapest collaboration [37] in the continuum limit, using the Taylor method, but with a physical box size L that is half the value of that of the other two calculations. There is a striking tension between the green bands and the other two results, which makes one conclude that the $N_\tau = 8$ results from the HotQCD collaboration are probably effected by large cut-off effects. On the other hand, agreement between the black point and the orange bands below $T = 145$ MeV indicate that in this range (which is the most relevant range for the CEP search) the finite volume effects are already negligible for the smaller volume result from Ref. [37]. The lattice results are compared with the prediction from the hadron resonance gas (HRG) model (solid black line). We can conclude that the Taylor coefficients up to 8th order are in good agreement with the HRG model for all temperatures below $T \approx 145$ MeV, as long as the continuum limit is taken².

Since the HRG is a non-critical model, often used as a noncritical baseline for comparisons, it is safe to say that as long as the continuum limit is taken, current lattice data show no

²Since corrections to the HRG model are expected to be exponentially suppressed at small T [38] agreement for the range available on the lattice implies that χ_6^B and χ_8^B will likely also agree with the HRG at lower temperatures.

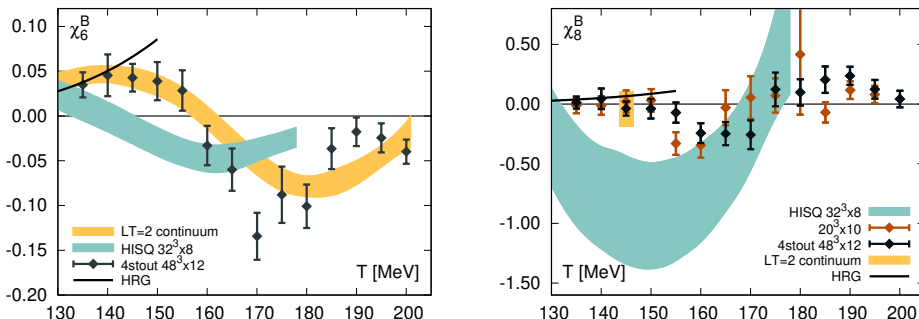


Figure 3. 6th (left) and 8th order baryon number fluctuations (right) at vanishing chemical potential from different lattice calculations (see main text). Solid black lines show predictions of the HRG model.

sign of the CEP. Let me warn the reader here, that this does not imply that the CEP does not exist. It is also a possibility, that it exists, but its effects on coefficients up to χ_8^B are smaller than the current error bars, or that its effects are only substantial for higher order coefficients.

Finally, let me note that there have been attempts to extract the position of the leading singularity of the QCD free energy from lattice QCD data [39–42], with the hope of eventually arriving at a prediction for the critical endpoint position. Unfortunately, these calculations have all been based on lattice QCD results on coarse lattices. Considering the rather large cut-off effects at $\mu_B > 0$, which can be seen, e.g., in the green bands of Fig. 3., these works are at the moment only of technical interest to lattice practitioners, and don't have any solid indications for heavy ion phenomenology.

4 The equation of state, isentropes and critical lensing

The most straightforward way of estimating the equation of state of hot-and-dense QCD matter is via a straightforward substitution to eq. (2). At order χ_4^B , this gives accurate results for about $\mu_B/T < 2$ [43]. Going to order χ_8^B extends this range up to at least $\mu_B/T = 3$ [43]. Alternatively, one can use the lower order coefficients χ_2^B and χ_4^B and their temperature independence to calculate a resummation of the Taylor series (an alternative expansion scheme), introduced in Refs. [24, 26]. The resummation scheme is based on the existence of the approximate scaling variable in Fig. 2, but also allows for taking into account small deviations from this scaling. This resummation also is accurate at least to $\mu_B/T = 3$ [43], but potentially even higher, since unlike a truncated Taylor expansion, conditions of thermodynamic stability in this case are manifest [24]. Recent results from the Taylor expansion can be found in Ref. [36] and from the discussed resummed expansion in Ref. [26]. Both of these works take into account the strangeness neutrality condition $n_S = 0$. Ref. [26] also gives the equation of state for a small non-zero value of the strangeness density n_S , which allows practitioners of hydrodynamic simulations to take into account local fluctuations of the strangeness density.

One application of the equation of state is the calculation of isentropes: curves of constant entropy density to baryon density ratio s/n_B in the $T - \mu_B$ plane. Near the CEP, they are expected to show the phenomena of critical lensing [44, 45]: the CEP pulls the isentropes towards itself, increasing their local density in the critical region. Fig. 4 shows the isentropes from the resummation/alternative expansion scheme. While the alternative scheme can reach larger values of μ_B , the qualitative conclusion from the Taylor expansion and the resummation are the same: within errors, and within covered values of μ_B , there is no critical lensing. The

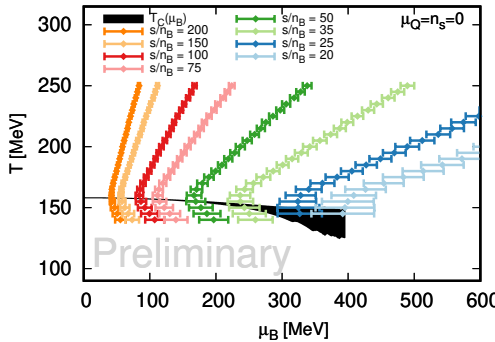


Figure 4. Isentropes of the T - μ_B plane from the alternative expansion scheme of Refs. [24, 26].

largest density isentrope, with $s/n_B = 20$ roughly corresponds to the smallest collision energy available in the RHIC Beam Energy scan [46, 47].

5 Summary and outlook

I have discussed lattice QCD calculations of the QCD phase diagram. Currently lattice results are available in a range of baryochemical potentials that roughly overlaps with the experimental range of the RHIC Beam Energy Scan (in collider mode). Thus, in spite of the difficulty of the sign problem, first-principles theory has mostly managed to keep up with the experimental effort. This is in part due to an increase in the available computational resources, and in part due to the invention of new extrapolation techniques, such as the alternative expansion scheme/resummation of Refs. [24, 26]. Continuum extrapolated lattice QCD results lead to a rather consistent picture: a crossover transition with a temperature that is μ_B dependent, but with a width that is approximately constant in μ_B for at least most of the range of the RHIC Beam Energy Scan. While the state-of-the-art lattice results do reach the end of the RHIC range, at the largest densities, the errorbars start to increase. E.g., while there is no sign of critical lensing in Fig. 4, the current error bars do allow for some of it for the largest densities reached at RHIC in collider mode. Thus, results from phase II of the RHIC Beam Energy Scan should be interesting, as they will shed some light on the position of the coveted critical endpoint. For theory to also keep up with future experiments, where considerably larger densities will be studied, theoretical/calculational innovations will be necessary. Such developments will be a priority for the lattice QCD community in the coming years.

Acknowledgements

Supported by the Hungarian National Research, Development and Innovation Office, NKFIH Grant No. KKP126769 and by the NKFIH excellence grant TKP2021_NKTA_64 and under Project No. FK 147164.

References

- [1] Y. Aoki et al., Nature **443**, 675 (2006), [hep-lat/0611014](https://arxiv.org/abs/hep-lat/0611014)
- [2] S. Borsányi et al., Phys. Lett. B **730**, 99 (2014), [1309.5258](https://arxiv.org/abs/1309.5258)

- [3] A. Bazavov et al. (HotQCD), Phys. Rev. D **90**, 094503 (2014), [1407.6387](#)
- [4] S. Borsanyi et al., Nature **539**, 69 (2016), [1606.07494](#)
- [5] P. Kovács, Z. Szép, G. Wolf, Phys. Rev. D **93**, 114014 (2016), [1601.05291](#)
- [6] R. Critelli et al., Phys. Rev. D **96**, 096026 (2017), [1706.00455](#)
- [7] P. Isserstedt et al., Phys. Rev. D **100**, 074011 (2019), [1906.11644](#)
- [8] W.j. Fu et al., Phys. Rev. D **104**, 094047 (2021), [2101.06035](#)
- [9] M. Marczenko, K. Redlich, C. Sasaki, Phys. Rev. D **107**, 054046 (2023), [2301.09866](#)
- [10] S. Borsányi et al. (Wuppertal-Budapest), JHEP **09**, 073 (2010), [1005.3508](#)
- [11] A. Bazavov et al., Phys. Rev. D **93**, 114502 (2016), [1603.06637](#)
- [12] S. Borsanyi et al., Phys. Rev. Lett. **125**, 052001 (2020), [2002.02821](#)
- [13] A. Andronic et al., Nature **561**, 321 (2018), [1710.09425](#)
- [14] A. Andronic et al., Phys. Lett. B **792**, 304 (2019), [1808.03102](#)
- [15] F.A. Flor, G. Olinger, R. Bellwied, Phys. Lett. B **814**, 136098 (2021), [2009.14781](#)
- [16] F.A. Flor, G. Olinger, R. Bellwied, Phys. Lett. B **834**, 137473 (2022), [2109.09843](#)
- [17] P. Braun-Munzinger et al., Phys. Lett. B **596**, 61 (2004), [nucl-th/0311005](#)
- [18] A. Pásztor, Z. Szép, G. Markó, Phys. Rev. D **103**, 034511 (2021), [2010.00394](#)
- [19] C. Bonati et al., Phys. Rev. D **92**, 054503 (2015), [1507.03571](#)
- [20] R. Bellwied et al., Phys. Lett. **B751**, 559 (2015), [1507.07510](#)
- [21] C. Bonati et al., Phys. Rev. D **98**, 054510 (2018), [1805.02960](#)
- [22] A. Bazavov et al. (HotQCD), Phys. Lett. B **795**, 15 (2019), [1812.08235](#)
- [23] S. Floerchinger, C. Wetterich, Nucl. Phys. A **890-891**, 11 (2012), [1202.1671](#)
- [24] S. Borsányi et al., Phys. Rev. Lett. **126**, 232001 (2021), [2102.06660](#)
- [25] S. Borsanyi et al., Phys. Rev. D **105**, L051506 (2022), [2108.09213](#)
- [26] S. Borsányi et al., Phys. Rev. D **105**, 114504 (2022), [2202.05574](#)
- [27] A. Majumder, B. Muller, Phys. Rev. Lett. **105**, 252002 (2010), [1008.1747](#)
- [28] A. Bazavov et al., Phys. Rev. Lett. **113**, 072001 (2014), [1404.6511](#)
- [29] P. Alba et al., Phys. Rev. D **96**, 034517 (2017), [1702.01113](#)
- [30] A. Bzdak, V. Koch, V. Skokov, Phys. Rev. C **87**, 014901 (2013), [1203.4529](#)
- [31] P. Braun-Munzinger et al., Nucl. Phys. A **1008**, 122141 (2021), [2007.02463](#)
- [32] V. Vovchenko et al., Phys. Lett. B **811**, 135868 (2020), [2003.13905](#)
- [33] M. D'Elia, G. Gagliardi, F. Sanfilippo, Phys. Rev. D **95**, 094503 (2017), [1611.08285](#)
- [34] S. Borsányi et al., JHEP **10**, 205 (2018), [1805.04445](#)
- [35] A. Bazavov et al., Phys. Rev. D **101**, 074502 (2020), [2001.08530](#)
- [36] D. Bollweg et al. (HotQCD), Phys. Rev. D **105**, 074511 (2022), [2202.09184](#)
- [37] S. Borsányi et al. (2023), [2312.07528](#)
- [38] R. Dashen, S.K. Ma, H.J. Bernstein, Phys. Rev. **187**, 345 (1969)
- [39] M. Giordano, A. Pásztor, Phys. Rev. D **99**, 114510 (2019), [1904.01974](#)
- [40] M. Giordano et al., Phys. Rev. D **101**, 074511 (2020), [1911.00043](#)
- [41] P. Dimopoulos et al., Phys. Rev. D **105**, 034513 (2022), [2110.15933](#)
- [42] G. Basar (2023), [2312.06952](#)
- [43] S. Borsányi et al., Phys. Rev. D **107**, L091503 (2023), [2208.05398](#)
- [44] C. Nonaka, M. Asakawa, Phys. Rev. C **71**, 044904 (2005), [nucl-th/0410078](#)
- [45] T. Dore et al., Phys. Rev. D **106**, 094024 (2022), [2207.04086](#)
- [46] L. Adamczyk et al. (STAR), Phys. Rev. C **96**, 044904 (2017), [1701.07065](#)
- [47] J. Adam et al. (STAR), Phys. Rev. Lett. **126**, 092301 (2021), [2001.02852](#)